

Polar Smectic Films

Isabelle Kraus* and Robert B. Meyer

The Martin Fisher School of Physics, Brandeis University, Waltham, Massachusetts 02254-9110

(Received 27 October 1998)

We report on a new experimental procedure for forming and studying polar smectic liquid-crystal films. A free-standing smectic film is put in contact with a liquid drop, so that the film has one liquid-crystal/air interface and one liquid-crystal/liquid interface. This polar environment results in changes in the orientational order parameter textures observed in the film, including a boojum texture and a previously unobserved spiral texture in which the winding direction of the spiral reverses at a finite radius from its center. Some aspects of these textures are explained by the presence of a K_{sb} term in the bulk elastic free energy that favors a combination of splay and bend curvatures. [S0031-9007(99)09072-9]

PACS numbers: 61.30.Gd, 07.05.Tp, 47.54.+r

Interfaces have a strong influence on molecular ordering, especially in soft condensed phases of organic molecules. This is most evident for thin films from a few to a few hundred nanometers thick. In particular, interfacial interactions can be employed to create a polar environment for a thin film, by placing it between two different isotropic media, liquid at one interface and air at the other. Illustrations include biphasic systems, e.g., prewetting films which form at the surface of a mesogenic liquid [1], as well as biochemical systems where the liquid medium is chemically different from the ordered wetting phase. These include nematic films spread on glycerin [2], as well as Langmuir multilayer [3] and monolayer [4] films spread on water. For polar and nonpolar films with in-plane orientational order, such as a two dimensional (2D) nematic or hexatic phase, a fascinating aspect of these self-organizing systems is the orientational patterns, or textures, they adopt, both in unbounded geometries and in 2D confined domains. Confinement imposes topological constraints, often forcing the formation of defects, such as point disclinations, in the observed textures. Understanding the delicate balance of forces that dictates the equilibrium textures has proved to be a challenging problem that has received a great deal of attention in the literature. For instance, the energetics governing the location of, and texture around, a single point disclination in a circular domain has been a long-standing theoretical problem [5] on which recent progress has been made [6,7].

In this Letter, we report a new experimental method for creating a polar environment for a thin film, starting with a free-standing film of smectic liquid-crystal (LC) material, and depositing it onto a liquid drop by contact (see Fig. 1). This method makes use of much simpler techniques and smaller scale apparatus than the ones commonly used to study Langmuir films, for example. It also provides researchers with a broad range of experimental possibilities such as wetting the film with any kind of liquid, as long as it does not dissolve the liquid crystal, and choosing the initial thickness of the film. We developed this technique especially to study the changes in

texture observed when a free-standing film was put into a polar environment. We examined films of the tilted chiral smectic C^* ($Sm C^*$) phase of several liquid crystals on a variety of liquid substrates. We paid particular attention to single circular domains in which we observed significant changes in the textures of the in-plane orientational order parameter involving a topological point disclination, including a boojum pattern (Fig. 2c) [8] and, most remarkably, a spiral pattern reversing its direction of winding at a particular radius (Fig. 2b). We also discovered the importance of a previously unutilized term in the free energy for these systems that favors an equilibrium state with combined splay ($\nearrow \uparrow \nwarrow$) and bend ($\nearrow \longrightarrow \searrow$) curvatures.

We start with a free-standing film of a thermotropic smectic, formed by spreading the smectic across a circular frame (a 6 mm diameter hole in a thin metal plate). The film consists of a stack of molecular layers, each about 3 nm thick, oriented parallel to the two free surfaces in contact with air, defining a film of homogeneous thickness. Using a micrometer screw, the film is lowered toward the top of a liquid drop. The drop (of, say, water) is held in place in a small hydrophilic circle on an otherwise hydrophobically treated glass substrate. When the contact is established, the resulting sample consists of the polar film itself as shown in Fig. 1 and of the “remaining” free-standing film stretched between the film holder and the liquid medium. On the drop, a circular meniscus of extra LC material forms at the junction of the free-standing film with the polar film. Depending on the relative surface tensions of the three surfaces meeting at this meniscus, the top of the drop is flatter than initially, still tending to be somewhat curved. The diameter of the polar film can be varied by raising or lowering the film holder.

The original free-standing film can be made in thicknesses ranging from thousands down to two layers [9]. We made samples of hundreds of layers, down to about 30 layers. Extremely thin samples are difficult to deposit by this method. We examined films on distilled water, glycerol, ethylene glycol, and aqueous solutions of

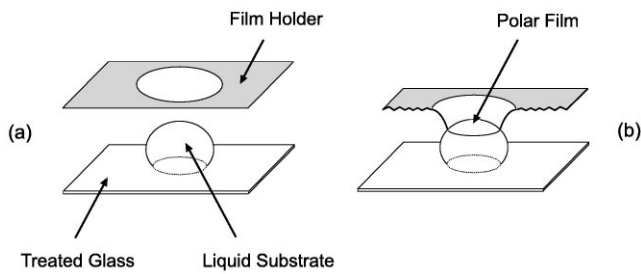


FIG. 1. Experimental setup: (a) Before contact, a free-standing film is spread on the holder and a drop of liquid is deposited on the slide. (b) After contact, the polar film is created on top of the drop.

poly-vinyl-alcohol and sodium dodecyl sulfate. We ran the experiment at 20 °C in order to minimize the evaporation of the wetting liquid. Most of our studies were made on films of the room temperature ferroelectric $Sm C^*$ mixture CS1015 from Chisso [10].

$Sm C^*$ is a layered liquid-crystal phase composed of chiral (nonreflection symmetric) molecules. The mean molecular long axis, given by the director \hat{n} , chosen to point “upwards” from the film, is tilted relative to the layer normal through an equilibrium angle ψ (26° for CS1015). The projection of \hat{n} onto the plane of the film defines the unit vector field, the c director $\hat{c}(x, y)$. The chirality of $Sm C^*$ results in a spontaneous rotation of \hat{c} as a function of z , the direction normal to the plane of the film. Given the helix pitch of the $Sm C^*$ phase for CS1015 of 3 μm , and our maximum film thickness of a few hundred nm, we neglect this effect and we consider $\hat{c}(x, y)$ uniform through the film thickness [11].

The samples were examined both under a polarizing transmission microscope (PTM) to study the texture of the c director, and under a white light reflection microscope to observe their thickness. The images were recorded by a CCD camera and image processing hardware to amplify small differences of intensity. With crossed polarizers, the

film image in the PTM is marked by dark brushes when the vector $\hat{c}(x, y)$ is parallel to either polarizer, and by bright brushes when \hat{c} is at an intermediate orientation. Thus, a cross-shaped four-arm extinction pattern (Fig. 2a) represents one full rotation of \hat{c} around a point defect, with a 45° rotation of \hat{c} between dark and bright areas. Because we slightly uncrossed the polarizers (a few degrees) to increase light intensity, the dark/bright sequence in Figs. 2b and 2c corresponds to a 90° rotation of \hat{c} .

Upon forming the polar film, in a few square mm we see hundreds of edge dislocation loops defining domains of different thickness throughout the area of the film. These domains, roughly circular, are practically static. Moreover, the domains are not isolated from each other, but are packed together, so they resemble a foam, rather than free circular regions [12]. We have observed many new textures in the resulting polar films, some involving transitions to other smectic phases. In all the cases discussed here, our observation of rapid fluctuations of the c director convinced us that samples were in the $Sm C^*$ phase.

Within a domain we can compare the c -director texture to that observed in the circular islands (thicker regions) seen in nonpolar free-standing films. The circular topology of an island or a domain, together with a strong anchoring of the c director at a fixed angle relative to the boundary, combine to produce a topological constraint, resulting in the existence of a point disclination in the domain, around which the c director rotates once. The detailed texture within the domain, including the location of the disclination, is dictated by the free energy for the c director. This includes anchoring energies at the outer boundary and around the point defect, and the curvature elastic energy for gradients of the c director within the domain. Following the detailed symmetry analysis presented by Langer and Sethna [5], the elastic free energy F for the c director in a chiral polar thin film, averaged over the film thickness, has the form

$$F = \int_{\text{area}} dA [K_s (\nabla \cdot \hat{c})^2 + K_{sb} (\nabla \cdot \hat{c}) (\nabla \times \hat{c}) + K_b (\nabla \times \hat{c})^2] + \oint_{\text{boundary}} dl [\lambda_s (\hat{c} \cdot \hat{m}) + \lambda_b (\hat{c} \times \hat{m})],$$

in which K_s and K_b are the familiar splay ($\nabla \cdot \hat{c} \sim \searrow \uparrow \swarrow$) and bend ($\nabla \times \hat{c} \sim \swarrow \rightarrow \searrow$) curvature elastic constants, λ_s and λ_b give the strength of the lowest

order terms dictating the c -director anchoring at the domain boundary, and \hat{m} is the outward normal to the boundary. For 2D vectors, the \times operation produces a

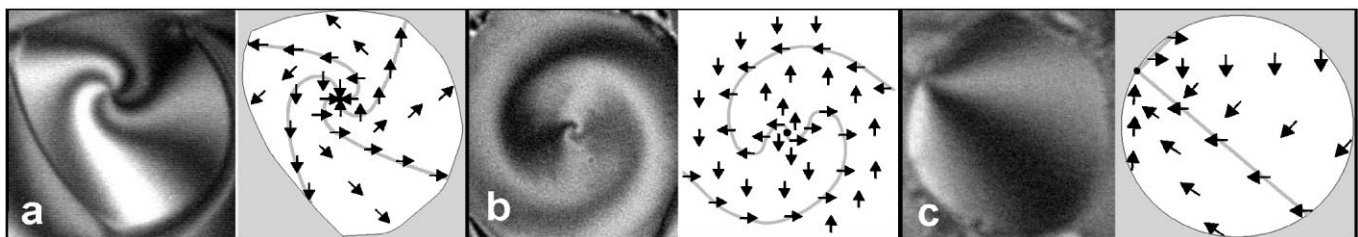


FIG. 2. Textures and sketches of director patterns, observed between (a) crossed and [(b), (c)] slightly uncrossed (vertical and horizontal) polarizers. Each image is about 50 μm wide. (a) Simple spiral. (b) Reversing spiral. (c) Boojum.

scalar. The cross term in splay and bend, which is unique to films that are both chiral and polar, has special stability requirements: K_{sb} can be positive or negative, but to make the free energy density positive definite for arbitrary values of splay and bend, we require that $K_{sb}^2 < 4K_sK_b$. The K_s and K_b terms could have been written to include spontaneous splay and bend in the ground state [13], but those added terms can be integrated by parts to combine with the λ_s and λ_b terms.

This free energy expression represents an average of the molecular interactions through the thickness of the film, including the surfaces and the interior of the film. The relative magnitudes of the coefficients of different terms depend on the nature of the molecules and their interactions, and on the molecular tilt angle ψ . Since the texture depends on a competition among various terms in the free energy, many textures are possible. Since we are focusing on polar effects, the magnitudes of the two polar coefficients K_{sb} and λ_s are important. They arise only from the surface layers of the film, which are naturally polar. In a free-standing film in air, because of the top-bottom symmetry, the exactly opposite polarities of the two surfaces cancel, making the polar coefficients identically zero, while in our samples on the liquid surface, this symmetry is broken. However, the net polarity arises only from the surface layers, so the magnitude of the polar coefficients, compared to the coefficients arising from interactions in the interior of the film, is inversely proportional to the film thickness, making that a useful variable for tuning polarity.

Focusing first on a nonpolar free-standing film, the λ_b term, which arises from chirality, favors one direction of tangential orientation of the c director at the boundary of a circular island. If $K_b < K_s$ [14], then a simple minimum energy texture is one of pure bend, with azimuthal orientation of \hat{c} within the circle and the point defect at its center. This highly symmetric texture, often seen in islands on free-standing films [15,16], is characterized by a cross-shaped four-brush extinction pattern, similar to that seen near the point defect in Fig. 2a but with straight brushes, when viewed between crossed polarizers.

In the case of a polar film, this simple texture is no longer observed, and other textures of the same topology are seen, the boojum texture (Fig. 2c) with a point defect located at the edge of the domain and straight brushes emerging radially from the defect, and several different spiral textures (Figs. 2a and 2b), including the “reversing spiral” with a centered defect around which the c -director field winds first one way and then the other, as a function of radius. In thinner films, the boojum texture is very commonly seen, while spirals are dominant in thicker samples; this may reflect differences in the strength of the polar perturbation. The reversing spiral is rare. To understand certain aspects of these textures, we look to the broken polar symmetry. The two polar terms, with coefficients K_{sb} and λ_s , break symmetry in different ways.

First, by itself the λ_s term would favor either inward or outward orientation of \hat{c} at a boundary. Combined with the λ_b term it selects one oblique orientation angle ϕ^* of the c director with respect to \hat{m} , rather than tangential or normal orientation. This oblique boundary condition is clearly seen in the domains of Figs. 2a and 2c, where a dark brush, corresponding to loci of horizontal \hat{c} , meets the domain boundary at the lower right, where it is oriented obliquely, rather than horizontally or vertically (see the accompanying sketches of the director patterns).

Second, the K_{sb} term, noted first by Langer and Sethna [5], but never used previously to analyze textures, appears only with both chiral and polar symmetry. This term lowers the symmetry of a texture because it favors combined splay and bend deformations. For a circular domain with a centered point defect at $r = 0$, instead of pure splay (\hat{c} radial, when $K_s < K_b$) or pure bend (\hat{c} azimuthal, when $K_b < K_s$) being the lowest energy distortion, a particular ratio of splay to bend minimizes the energy. In the absence of boundary anchoring conditions, this would lead to a simple spiral texture, with the c director making a constant angle $\phi = \phi_{sb}$ (or $\phi_{sb} + \pi$), with respect to the radial vector throughout the domain.

Combining these two symmetry breaking effects, it is clear why various spiral patterns are observed when the point defect is centered in a circular domain of a polar chiral film. At the outer boundary of the domain ($r = R$), the c director is anchored at some angle $\phi^* = \phi_b$. At the inner boundary defined around the point defect ($r = \epsilon$), the anchoring angle is $\phi^* = \phi_d$, which need not be the same as ϕ_b . Simultaneously, away from the boundaries, ϕ would tend to approach ϕ_{sb} . The energy minimizing texture requires that ϕ is a function of radius r in the domain. To find this functional dependence, one can make a transformation from polar (r, θ) to Cartesian (ξ, θ) coordinates, with $\xi = \ln(r/\epsilon)$. The circular domain is thereby mapped onto a strip of $\text{Sm } C^*$ contained between two parallel lines, $\xi = 0$ and $\xi = \ln(R/\epsilon)$, at which the boundary conditions on ϕ are ϕ_d and ϕ_b , respectively. The curvature energy which arose from the circular geometry of the domain transforms into a term in the free energy for the strip that can be thought of as arising from an effective uniform magnetic field parallel to the ξ, θ plane, oriented at angle ϕ_{sb} relative to the ξ axis. The director would tend to lie parallel to this magnetic field in the absence of other forces. The strength of the effective field coupling depends on relative magnitudes of the elastic constants. Often, this leads to solutions in which ϕ varies monotonically from ϕ_d to ϕ_b across the strip, corresponding to ordinary spirals for the brushes observed in our experiments (Fig. 2a). However, much as in the well-studied Fredericks transition in nematic layers [17], the solution can involve ϕ first rotating in one direction (from ϕ_d toward ϕ_{sb}) as a function of ξ , reaching an extremum, and then rotating in the other direction to

match the second boundary condition, ϕ_b . This produces the reversing spiral (Fig. 2b).

The straight brushes emerging from the defect in the boojum texture (Fig. 2c) are in contrast to the spiral patterns described above. Extending the results of Langer and Sethna [5], one can find a stable energy minimizing solution which produces the observed straight brushes and constant ϕ_b at the outer domain boundary. In terms of polar coordinates (r, θ) centered on the point defect, and ϕ again an angle relative to the radial vector, a stable solution is $\phi = \theta + \phi_b$, independent of r . This solution, in a circular domain of radius r_0 centered at the point $(r_0, 0)$ remarkably has the fixed angle ϕ_b between \hat{c} and \hat{m} at all points on the boundary of the domain (see the sketch of the director pattern for Fig. 2c). This is just the structure we see, subject to perturbations from the noncircular shape of the domains.

This boojum is similar to the topological defect texture observed in isolated domains of other systems, like Langmuir monolayers on water [6–8,18], which are also polar, and islands of the smectic *I* phase in an otherwise smectic *C* free-standing film [5]. In those systems the anchoring of the *c* director at the lateral boundary is weak, and the “virtual” topological defect has been “expelled” from the domain. That is, the brushes as seen in Fig. 2c would converge toward a point just outside the domain boundary. This lowers the free energy by removing the high elastic strain near the defect as well as its core energy, and by replacing it with a lower energy that results from the violation of the boundary anchoring in a small region. However, in our polar films, the boundary anchoring of the *c* director is apparently stronger, and the defect appears to be right at the edge of the domain. We speculate that this strong anchoring results from the large change in layer thickness at the domain boundaries of our polar films.

In conclusion, we have developed a novel technique for studying polar smectic films, and have observed novel textures in smectic *C** films in a polar environment. The flexibility of this technique, in varying the choice of liquid-crystal and liquid-substrate materials, and thickness of the smectic layer, should augment what we have learned about textures from observations of both free-standing films and Langmuir monolayers. We have shown through a free energy analysis that important aspects of the changes in texture relative to ordinary free-standing smectic *C** films are a direct consequence of the polar symmetry of the films.

We thank Jay Patel, Darren Link, and Noel Clark for providing us with chemical compounds. I.K. is grateful

to the city of Strasbourg for financial support through a Strasbourg-Boston twin cities fellowship. This research was supported by the NSF through Grant No. DMR-9415656 and by the Martin Fisher School of Physics at Brandeis University.

*Permanent address: Institut de Physique et Chimie des Matériaux, 23 rue du Loess, F-67037 Strasbourg Cedex, France.

- [1] R. Luth, Ch. Bahr, G. Heppke, and J.W. Goodby, *J. Chem. Phys.* **108**, 3716 (1998); V. Candel and Y. Galerne, *Phys. Rev. Lett.* **70**, 4083 (1993).
- [2] For a review see O.D. Lavrentovich and V.M. Pergamenschik, *Int. J. Mod. Phys. B* **9**, 2389 (1995).
- [3] B. Rapp and H. Gruler, *Phys. Rev. A* **42**, 2215 (1990).
- [4] For a review see C.M. Knobler, *Physica (Amsterdam)* **236A**, 11 (1997); Y. Tabe, N. Shen, E. Mazur, and H. Yokoyama, *Phys. Rev. Lett.* **82**, 759 (1999).
- [5] S.A. Langer and J.P. Sethna, *Phys. Rev. A* **34**, 5035 (1986).
- [6] Kok-Kiong Loh and Joseph Rudnick, *Phys. Rev. Lett.* **81**, 4935 (1998).
- [7] David Pettey and T.C. Lubensky, *Liq. Cryst.* **25**, 579 (1998).
- [8] T.M. Fisher, R.F. Bruinsma, and C.M. Knobler, *Phys. Rev. E* **50**, 413 (1994).
- [9] For a full description of the method see I. Kraus, P. Pieranski, E. Demikhov, H. Stegemeyer, and J. Goodby, *Phys. Rev. E* **48**, 1916 (1993).
- [10] The bulk phase sequence for CS1015 is Cr (−17 °C) Sm *C** (57 °C) Sm *A* (68 °C) *N** (78 °C) iso.
- [11] This statement is confirmed by experiments done with SCE10 sold by Merck [Sm *I* (−20 °C) Sm *C** (61 °C) *N** (109 °C) iso], which has a pitch of 14.6 μm, 5 times larger than CS1015. It exhibits patterns very similar to those seen in CS1015.
- [12] P. Pieranski *et al.*, *Physica (Amsterdam)* **194A**, 36 (1993); J-C. Geminard, R. Holyst, and P. Oswald, *Phys. Rev. Lett.* **78**, 1924 (1997).
- [13] R.B. Meyer and P.S. Pershan, *Solid State Commun.* **13**, 989 (1973).
- [14] C. Rosenblatt, R. Pindak, N.A. Clark, and R.B. Meyer, *Phys. Rev. Lett.* **42**, 1220 (1979).
- [15] C.D. Muzny and N.A. Clark, *Phys. Rev. Lett.* **68**, 804 (1992).
- [16] J.E. Maclennan, U. Sohling, N.A. Clark, and M. Seul, *Phys. Rev. E* **49**, 3207 (1994), Sec. IV.B.
- [17] P.G. de Gennes and J. Prost, *The Physics of Liquid Crystals* (Clarendon Press, Oxford, 1993), 2nd ed.
- [18] S. Riviere and J. Meunier, *Phys. Rev. Lett.* **74**, 2495 (1995).